Bioorganic & Medicinal Chemistry 21 (2013) 395–402

Contents lists available at SciVerse ScienceDirect

Bioorganic & Medicinal Chemistry

journal homepage: www.elsevier.com/locate/bmc

Ferrocene tripeptide Gly-Pro-Arg conjugates: Synthesis and inhibitory effects on Alzheimer's $A\beta_{1-42}$ fibrillogenesis and Aβ-induced cytotoxicity in vitro

Binbin Zhou [a,b], Chun-Lan Li [a], Yuan-Qiang Hao [a], Muya Chabu Johnny [a], You-Nian Liu [a,b,*], Juan Li [a,b,*]

[a] College of Chemistry and Chemical Engineering, Central South University, Changsha, Hunan 410083, PR China
[b] Key Laboratory of Resources Chemistry of Nonferrous Metals (Central South University), Ministry of Education, Changsha, Hunan 410083, PR China

ARTICLE INFO

Article history:
Received 26 July 2012
Revised 21 November 2012
Accepted 22 November 2012
Available online 2 December 2012

Keywords:
$A\beta_{1-42}$ fibrillogenesis
Ferrocene
GPR
Inhibitor
Cytotoxicity

ABSTRACT

Alzheimer's disease (AD) is the most common cause of dementia, and currently there is no clinical treatment to cure it or to halt its progression. Aggregation and fibril formation of β-amyloid peptides (Aβ) are central events in the pathogenesis of AD. Many efforts have been spent on the development of effective inhibitors to prevent Aβ fibrillogenesis and cause disaggregation of preformed Aβ fibrils. In this study, the conjugates of ferrocene and Gly-Pro-Arg (GPR) tripeptide, Boc-Gly-Pro-Arg(NO_2)-Fca-OMe (**4**, GPR–Fca) and Fc-Gly-Pro-Arg-OMe (**7**, Fc–GPR) (Fc: ferrocene; Fca: ferrocene amino acid) were synthesized by HOBT/HBTU protocol in solution. These ferrocene GPR conjugates were employed to inhibit $A\beta_{1-42}$ fibrillogenesis and to disaggregate preformed Aβ fibrils. The inhibitory properties of ferrocene GPR conjugates on $A\beta_{1-42}$ fibrillogenesis were evaluated by thioflavin T (ThT) fluorescence assay, and confirmed by atomic force microscopy (AFM) analysis. The interaction between the ferrocene GPR conjugates and $A\beta_{1-42}$ was monitored by electrochemical means. Our results showed that both GPR and GPR–Fca can significantly inhibit the fibril formation of $A\beta_{1-42}$, and cause disaggregation of the preformed fibrils. As expected, GPR–Fca shows stronger inhibitory effect on $A\beta_{1-42}$ fibrillogenesis than that of its parent peptide GPR. In contrast, Fc–GPR shows no inhibitory effect on fibrillogenesis of $A\beta_{1-42}$. Furthermore, GPR–Fca demonstrates significantly protection against Aβ-induced cytotoxicity and exhibits high resistance to proteolysis and good lipophilicity.

1. Introduction

Alzheimer's disease (AD) is a progressive and fatal neurodegenerative disorder in the elderly characterized by short-term memory loss, continuous cognitive decline and behavioral disturbances.[1] AD affects approximately 26.6 million population worldwide,[2] and the number of people with AD is increasing at a very high rate that there could be about 106.2 million by 2050,[3] resting an enormous burden on the family, health care and society. In the past two decades, a lot of effort has been spent to understand the pathogenesis of AD, in order to build a robust platform for effective pharmacological treatments. Although the precise mechanisms leading to neurodegeneration in AD are not fully understood yet, several pieces of evidence indicate that the conformational changes accompanying the aggregation and fibril formation of β-amyloid peptides (Aβ), might play a pivotal role in the pathogenesis of AD.[4] Therefore, one of the most attractive therapeutic targets for AD could rely on the use of the agents which could inhibit the fibril formation of Aβ or disaggregate the preformed Aβ fibrils.[5–8] A lot of progress has recently been made in design and synthesis of inhibitors for Aβ fibril formation.

To date, lots of structurally different compounds have been identified to prevent Aβ aggregation and/or disaggregate preformed fibrils. These compounds include small organic molecules and peptides or peptidomimetics.[6] Small molecules such as the antibiotic rifampicin,[9] 4′-iodo-4′-deoxydoxorubicin,[10] isaindigotone derivatives[11] and scyllo-inositol derivatives[12] have been found to prevent Aβ aggregation. Besides, peptides or peptidomimetic molecules, such as KLVFF and LPFFD show strong inhibition for Aβ misfolding and aggregation.[7,8,13] Glyprolines (Gly-Pro-Arg, GPRs) are the new family of regulatory peptides consisting of short glycine and proline-containing peptides,[14] which are produced in the organism during degradation and synthesis of elastin, collagen, and other connective tissue proteins.[15] Recently, GPR was employed to inhibit the development of AD.[14] For example, Uemura and coworkers found that GPR is a small neuroprotective peptide and can effectively prevent neuronal degeneration in vivo.[16] Thus, tripeptide GPR is considered as a potential lead compound for the treatment of AD. However, natural peptides as drug compounds are essentially limited by their poor membrane permeability and instability in blood plasma.

Ferrocene (Fc) and its derivatives exhibit a manifold of medicinal properties by serving as antimalarial, antibacterial and antitumor agents due to their biological activity, low cytotoxicity, high lipophilicity and unique electrochemical behavior.[17–21] Especially,

* Corresponding authors.
E-mail addresses: liuyounian@csu.edu.cn (Y.-N. Liu), juanli@csu.edu.cn (J. Li).

0968-0896/$ - see front matter © 2012 Elsevier Ltd. All rights reserved.
http://dx.doi.org/10.1016/j.bmc.2012.11.030

when incorporated into a drug, ferrocene moiety could yield interesting results.[22] For example, in the antimalarial compound oaferroquine[23] and the antitumor agent ferrocifen,[24] the introduction of the ferrocenyl moieties improves the activity of the compounds and alters their pharmacodynamic profiles. Recently, we conjugated ferrocene to pentapeptide KLVFF and found that Fc-KLVFF shows improved lipophilicity and significant resistance towards proteolytic degradation compared to its parent peptide, and high inhibitory effect towards the fibrillogenesis of $A\beta_{1-42}$.[25] Additionally, ferrocene peptide conjugates, synthesized by the route either from *C*-terminal or from *N*-terminal labelling, are recognized as useful tools in bioorganometallic chemistry.[26–28]

The main objective of this work is to combine the lipophilic nature and enzymatic stability of ferrocene moiety and the neuroprotective nature of GPR peptide, by designing and synthesizing several functional ferrocene GPR conjugates, and to investigate the effect of the conjugates on $A\beta_{1-42}$ fibrillogenesis and on the Aβ-induced toxicity towards human neuroblastoma SH-SY5Y cells.

2. Results and discussion

2.1. Synthesis and characterization of GPR–Fca and Fc–GPR

GPR tripeptide, one of the members of the glyproline family was found to possess the ability to protect and rescue cell death induced by Aβ.[16] As mentioned in the Introduction, the aim of this study is to design and synthesize of enzymatic resistance β-sheet breakers which can inhibit the $A\beta_{1-42}$ fibril formation and attenuate the Aβ-induced cytotoxicity. Ferrocene, due to its biological activity, low toxicity, and high lipophilicity may meet the requirement.[29,30] Moreover, the unique electrochemical behavior of ferrocene can be used to interrogate the interaction between β-sheet breakers and $A\beta_{1-42}$. Since the introduced bulky groups into tripeptide GPR may render steric hindrance, resulting in affecting the interaction with $A\beta_{1-42}$, ferrocene was attached to both *N*-terminal and *C*-terminal of GPR to investigate the effect on $A\beta_{1-42}$ fibril formation.

Both GPR–Fca and Fc–GPR were synthesized using HOBT/HBTU protocol in solution. (see Scheme 1). GPR–Fca and Fc–GPR were then characterized by FT-IR, ^{1}H NMR and ESI-MS (data were presented in detail in experimental procedures section), which indicating that ferrocene GPR conjugates were synthesized successfully. In order to highlight the role of Fc in this kind of β-sheet breaker, the tripeptide GPR was synthesized as a control.

2.2. Kinetics of fibril formation of $A\beta_{1-42}$ in the presence of ferrocene GPR conjugates

The binding of ThT to amyloid is specific, thus, ThT fluorescence assay has been extensively used to monitor the fibril formation of amyloid peptide.[31] Herein, the kinetics of fibril formation of $A\beta_{1-42}$ and the effects of ferrocene GPR conjugates on $A\beta_{1-42}$ fibrillogenesis were examined by ThT fluorescence assay. Typically, ThT fluorescence does not change when it binds to unstructured proteins. However, when it binds to aggregated amyloid, a new excitation peak at 450 nm and enhanced emission at 482 nm will be observed.

As shown in Figure 1, along with the incubation of $A\beta_{1-42}$ at a concentration of 25 μM alone at 32 °C, the ThT fluorescence increases exponentially for a period and then remains almost constant. Consistent with our previous studies, fibril formation of $A\beta_{1-42}$ starts at very short beginning, and reaches its plateau at the sixth day of incubation, after that, fluorescence intensity turns to saturation.[25] The equimolar composition of each inhibitor was co-incubated with $A\beta_{1-42}$, GPR and GPR–Fca show inhibitory effects on fibrillogenesis of $A\beta_{1-42}$, although to different extents. As seen from Figure 1, when $A\beta_{1-42}$ was incubated in the presence of GPR, the fluorescence intensity increases initially with incubation time, reaching its maximum at 4 days. However, a reduction in fluorescence intensity shows that GPR is able to inhibit the fibril formation of $A\beta_{1-42}$, in agreement with the neuroprotective behavior of GPR in vivo.[16] GPR–Fca exhibits similar ThT fluorescence pattern as that of GPR. Both GPR and GPR–Fca reveal significant inhibitory effects resulting in 40% and 50% reduction of the fibril formation, respectively. In contrast to GPR and GPR–Fca, Fc–GPR reveals negligible inhibitory effect on $A\beta_{1-42}$ fibrillogenesis. Our results point to robust inhibitory effects of GPR–Fca and GPR on $A\beta_{1-42}$ fibrillogenesis.

On the other hand, a control experiment was performed to test the self-aggregation of GPR–Fca and GPR using ThT fluorescence assay. A 25 μM GPR–Fca or GPR was incubated alone for 7 days at 32 °C in 0.1 M PBS (pH 7.4), respectively. No obvious ThT fluorescence was observed in either solution (data no shown), which suggests that neither GPR–Fca nor GPR undergoes self-aggregation in solution.

2.3. Concentration-dependent effects of ferrocene GPR conjugates on $A\beta_{1-42}$ fibrillogenesis

To investigate the concentration responses of GPR and ferrocene GPR conjugates on $A\beta_{1-42}$ fibrillogenesis, aliquots of $A\beta_{1-42}$ at a concentration of 25 μM were incubated with ferrocene GPR conjugates at 1:0.4, 1:1, 1:3, 1:5 and 1:10 ($A\beta_{1-42}$: GPR or ferrocene GPR conjugates, molar ratio). The ThT fluorescence assay was also exploited to monitor the formation of fibrils. As revealed by Figure 2, when $A\beta_{1-42}$ was incubated with different concentrations of GPR or GPR–Fca, the inhibition of amyloid fibril formation was apparently achieved and the inhibitory effect enhances rapidly with increasing dosage of inhibitors. Moreover, our results indicated that GPR–Fca is a more potent inhibitor of $A\beta_{1-42}$ fibrillogenesis than GPR. The IC_{50} values (the molar ratio of inhibitor to $A\beta_{1-42}$ fibrillogenesis with 50% maximum effect) for GPR and GPR–Fca are 3.28 ± 0.53 and 1.42 ± 0.31, respectively. We suggest that the difference in IC_{50} between GPR and GPR–Fca could be ascribed to the hydrophobicity of ferrocene which makes the GPR–Fca more easily to interact with $A\beta_{1-42}$. Furthermore, the introduction of ferrocenoyl moiety could act as a good disrupting element for $A\beta_{1-42}$ fibrillogenesis. In contrast, Fc–GPR shows no significant inhibition of fibrillogenesis upon the $A\beta_{1-42}$ even at a molar ratio of 1:10 and the IC_{50} values for Fc–GPR should be higher than 10.

2.4. Kinetics of the interaction between $A\beta_{1-42}$ and ferrocene GPR conjugates

An attractive therapeutic strategy for AD is to block the aggregation of Aβ by inhibitors which contain a recognition element and a disrupting element.[32] During the past decades, KLVFF peptide has been extensively used as a recognition element to devise inhibitors for Aβ fibrillation.[8,33] In our previous study, we devised an ferrocenoyl inhibitor for Aβ fibrillation depending on KLVFF and utilized the electrochemical method to study the interaction between Aβ and Fc–KLVFF according to the redox active properties of ferrocenoyl conjugate.[25] Here, the electrochemical properties of GPR–Fca and Fc–GPR were also investigated by cyclic voltammetry (CV). A pair of well-defined redox peaks, with the cathodic and anodic peak potentials at 552 mV and 478 mV versus Ag/AgCl, respectively, was observed for GPR–Fca, and the ratio of oxidative to reductive peak currents is close to unity, indicating electrochemical reversibility of the electrode process. Similarly, Fc–GPR also undergoes a reversible electron-transfer reaction (data not shown). Due to the excellent intrinsic electrochemical signals of the ferrocene GPR conjugates, differential pulse voltammetry

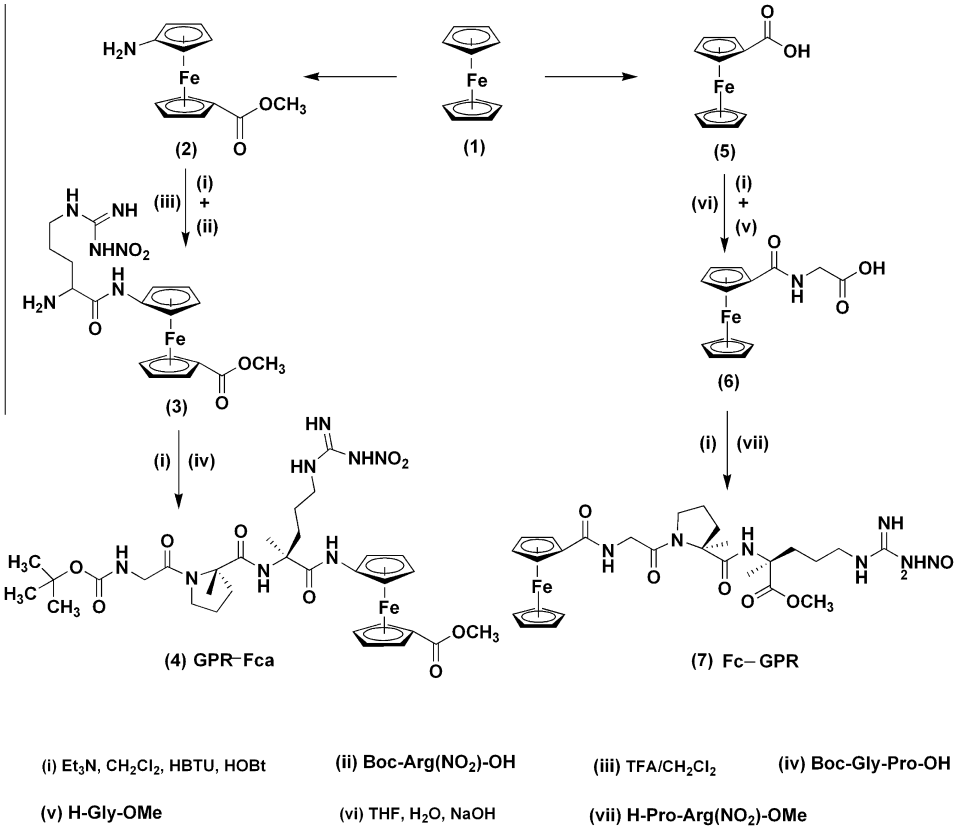

Scheme 1. Syntheses of ferrocene GPR conjugates.

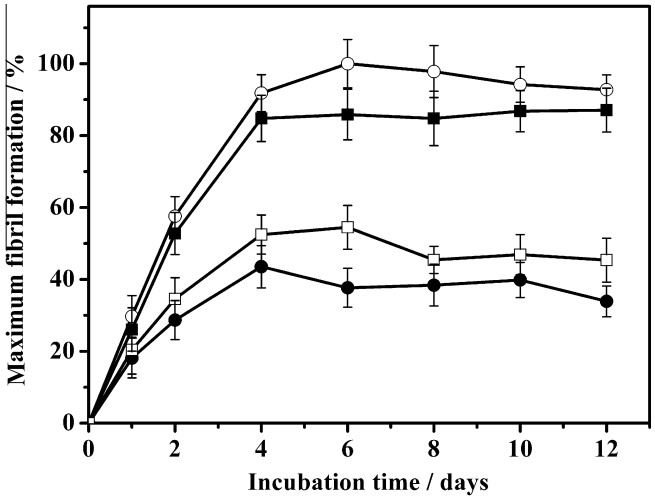

Figure 1. Inhibition of GPR peptide and ferrocene GPR conjugates on the kinetics of $A\beta_{1-42}$ fibrillogenesis. Twenty five micrometer freshly prepared $A\beta_{1-42}$ was incubated at 32 °C alone (○) or in the presence of 25 μM Fc–GPR (■), GPR (□), GPR–Fca (●) for the indicated times. Fibril formation was quantitated by the ThT fluorometry assay as described in methods. Data are expressed as a percentage of maximum fibril formation (fluorescence intensity). Each experiment was repeated three times ($n = 3$), and error bars represent the standard deviation (SD) of the fluorescence measurement.

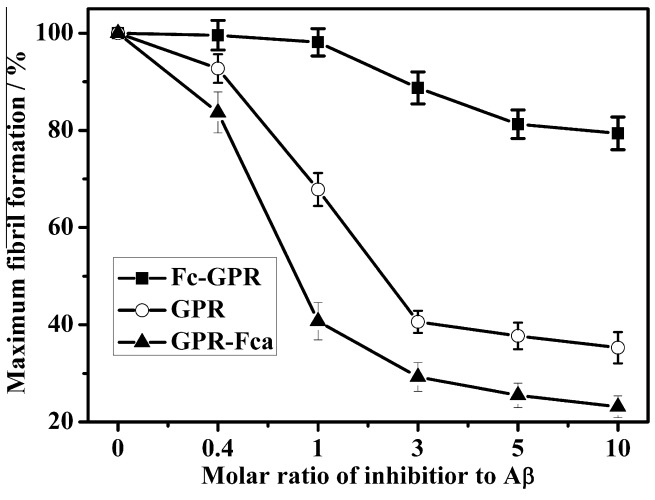

Figure 2. Concentration-dependent effect of GPR and ferrocene GPR conjugates on $A\beta_{1-42}$ fibrillogenesis. 25 μM freshly prepared $A\beta_{1-42}$ was incubated at 32 °C in the presence of GPR (○), Fc–GPR (■) or GPR–Fca (▲) of difference concentrations in 0.1 M PBS (pH 7.4) for 4 days. Reported data are expressed as a percentage of maximum fluorescence intensity. Data represent the mean ThT fluorescence measurement of three independent experiments ($n = 3$). Error bars represent the standard deviation (SD) of the fluorescence measurement.

(DPV) method was conducted to calculate the kinetics of the interaction between $A\beta_{1-42}$ and the ferrocene GPR conjugates. As shown in Figure 3, the DPV peak currents drop sharply when GPR–Fca was incubated with $A\beta1_{-42}$ in a very short time, suggesting that GPR–Fca is capable of interacting with $A\beta1_{-42}$ instantaneously. To exclude the current drops from the self-aggregation of GPR–Fca, the solution containing the same concentration of GPR–Fca in the absence of $A\beta_{1-42}$ was also monitored by the DPV, and the results shows the current remained unchanged for 6 h, suggesting that GPR–Fca does not undergo self-aggregation during this period. On the other hand, the current of Fc–GPR in the presence of $A\beta_{1-42}$ was monitored at various incubation times, and we observed that there were no significant changes in the peak currents. It is

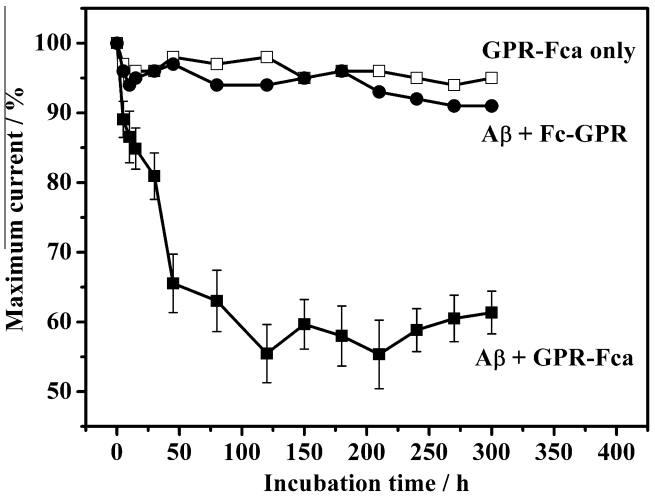

Figure 3. The kinetics of $A\beta_{1-42}$ fibrillogenesis in the present of ferrocene GPR conjugates by using DPV method. Fifty micrometer $A\beta_{1-42}$ was incubated in the presence of 50 μM Fc–GPR (●) or GPR–Fca (■) in PBS (pH 7.4) at 32 °C for the indicated times. Additionally, 50 μM GPR–Fca (□) was incubated alone under the same experimental conditions as a control experiment. Data are expressed as a percentage of the maximum anodic peak current of ferrocene GPR conjugates alone. The experiment of co-incubation of $A\beta_{1-42}$ with GPR–Fca was repeated three times ($n = 3$), and error bars represent the standard deviation (SD) of the current.

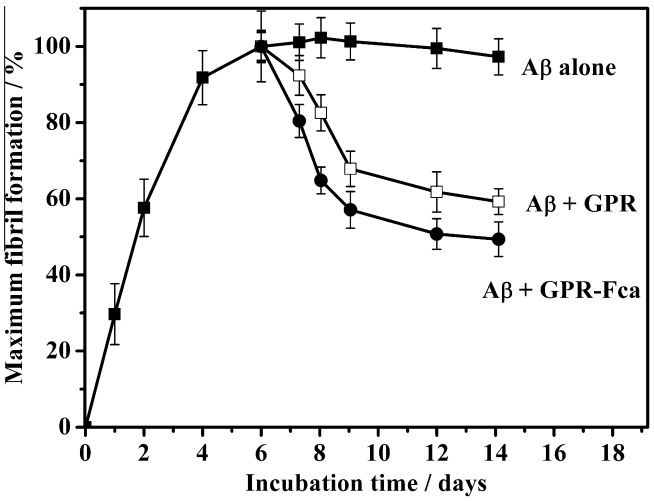

Figure 4. Disaggregation effect of preformed amyloid fibrils by GPR and GPR–Fca. Freshly prepared $A\beta_{1-42}$ at 25 μM was incubated alone in 0.1 M PBS at 32 °C for 6 days. A solution of GPR or GPR–Fca at 25 μM was then added to the preformed $A\beta_{1-42}$ fibril solution and incubated at 32 °C. Fibril concentration was quantitated by the ThT fluorescence assay, as described in Methods. Data are expressed as a percentage of maximum fibril formation (fluorescence intensity). Each experiment was repeated three times ($n = 3$), and error bars represent the standard deviation (SD) of the fluorescence measurement.

probably due to the attachment of ferrocene directly to the N-terminal of GPR causes steric hindrance, thus may hinder the interactions between GPR and $A\beta_{1-42}$.

2.5. Disaggregation effect of GPR and GPR–Fca on preformed $A\beta_{1-42}$ fibrils

To determine whether GPR–Fca or GPR can cause the disaggregation of mature $A\beta_{1-42}$ fibrils, we utilized GPR–Fca and GPR to treat the preformed $A\beta_{1-42}$ fibrils. The mature $A\beta_{1-42}$ fibrils were prepared by incubation of 25 μM $A\beta_{1-42}$ alone for 6 days at 32 °C, then equimolar of the inhibitor was added to the preformed fibril solution and co-incubated at 32 °C. As depicted in Figure 4, the maximum level of fibril disaggregation with these inhibitors was obtained after 5 days of incubation and remained unchanged thereafter. The result is similar to that of reported by Soto and coworkers.[34] GPR–Fca can efficiently induce disaggregation of $A\beta_{1-42}$ fibrils, achieving disaggregation of about 50% $A\beta_{1-42}$ fibril reduction after incubated for 5 days. Disaggregation of mature fibrils by 61% by GPR was observed too. Together, these results show GPR–Fca disaggregates mature fibrils in a more potent way than GPR.

2.6. Effect of GPR–Fca on $A\beta_{1-42}$ fibril morphology

AFM was used to image the morphologies of insoluble species produced in $A\beta_{1-42}$ solution as well as in the mixture of $A\beta_{1-42}$/GPR–Fca. As can be seen from Figure 5A, in the absence of GPR–Fca, $A\beta_{1-42}$ formed typical amyloid-like, 8-10 nm in length unbranched fine fibrils after 2 days incubation at 32 °C. The fibrils become more clearly visible after 6 days incubation (Fig. 5B), similar to our previous studies.[25] In contrast, in the presence of GPR–Fca, a lot of insoluble globular aggregates were observed after 2 days incubation, and a few larger aggregates (as shown in Fig. 5C, the size is about sub-micrometer) are exclusively of the amorphous morphology. As revealed by Figure 5D, the amount of the amorphous aggregates became greater after 6 days of incubation, and the protofibrils as well as any kind of fibrillar materials were absent completely. The images show dramatic difference between inhibitor-free $A\beta_{1-42}$ control sample and samples incubated with GPR–Fca. To exclude the self-aggregates of GPR–Fca, we incubated GPR–Fca solutions separately and used AFM to determine insoluble species that might have formed at various incubation times. There were no visible structures observed even after 7 days by the AFM (data not shown). It demonstrated again GPR–Fca was not self-aggregated and the amorphous aggregate was mainly contributed to the strong interaction between GPR–Fca and the intermediate aggregates of $A\beta_{1-42}$. The AFM results further confirmed GPR–Fca can inhibit $A\beta_{1-42}$ fibrillogenesis, in agreement with the ThT fluorescence results.

2.7. Effect of GPR–Fca and GPR on Aβ-induced cytotoxicity

Aggregated Aβ is revealed to be toxic to neurons and cause cognitive decline in AD patients. In this study, both ThT assay and AFM results showed that GPR–Fca and GPR inhibit the $A\beta_{1-42}$ fibril formation successfully. Previous studies on the inhibition of the fibril formation of Aβ showed that most (but not all) Aβ inhibitors have the potency to prevent the Aβ-induced cytotoxicity.[35–37] For instance, El-Agnaf and co-workers found that though both RGKLVFFGR and RGKLVFFGR-NH_2 are able to effectively inhibit Aβ fibril formation, only RGKLVFFGR-NH_2 can protect human neuroblastoma SH-SY5Y cells from Aβ toxicity.[38] Thus, we determined the effects of GPR and GPR–Fca on Aβ-induced toxicity towards human neuroblastoma SH-SY5Y cells by MTT assay.

Consideration that ferrocene is innocuous to many cell lines,[39] and consequently the ferrocene tag would not compromise the ability of GPR–Fca for alleviating the cytotoxicity inflicted by $A\beta_{1-42}$ aggregates. Thus, the human neuroblastoma SH-SY5Y cells were employed to investigate this consideration. As shown in Figure 6, the SH-SY5Y cells viability which was exposed to the pre-aggregated $A\beta_{1-42}$ exhibits only as 55%. At the molar ratio of 1:1 (GPR: $A\beta_{1-42}$), the mixture solution was pre-incubated under the same conditions, the treated cell viability was rescued to 80% which is consistent with the result in Uemura's work,[16] showing GPR prevents and rescues Aβ-induced neuronal apoptosis. When GPR–Fca was incubated with $A\beta_{1-42}$, the cell viability was rescued to 85% which is higher than the one treated with the GPR/$A\beta_{1-42}$ mixture, in good agreement with our ThT results (Figs. 1 and 2).

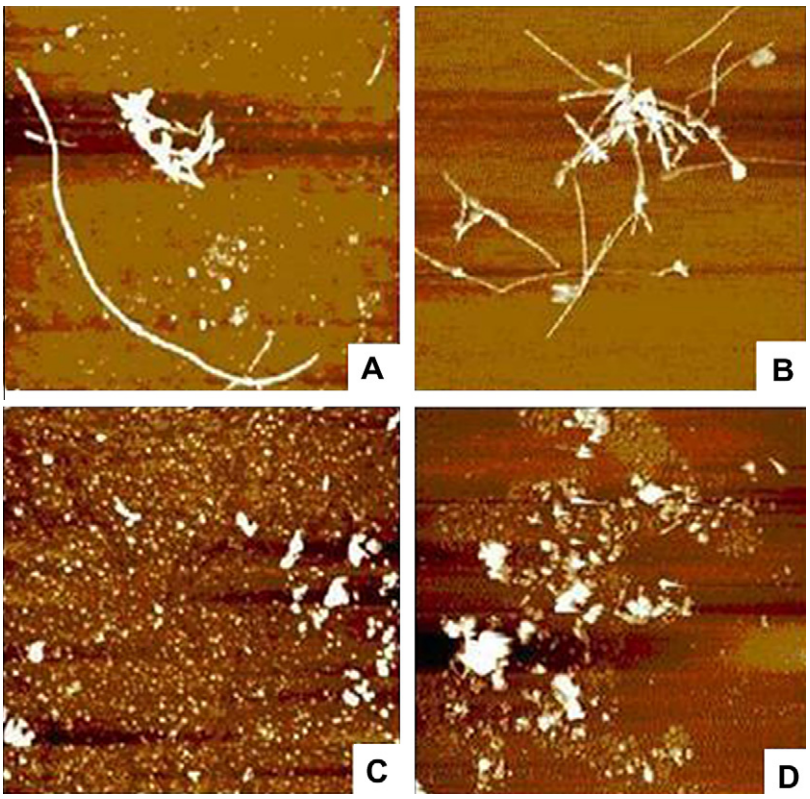

Figure 5. AFM observation of fibril formation. Aliquots of 25 μM $A\beta_{1-42}$ were incubated alone (top) or in the presence of 25 μM GPR–Fca (bottom) at 32 °C for 2 days (A, C) and 6 days (B, D), respectively.

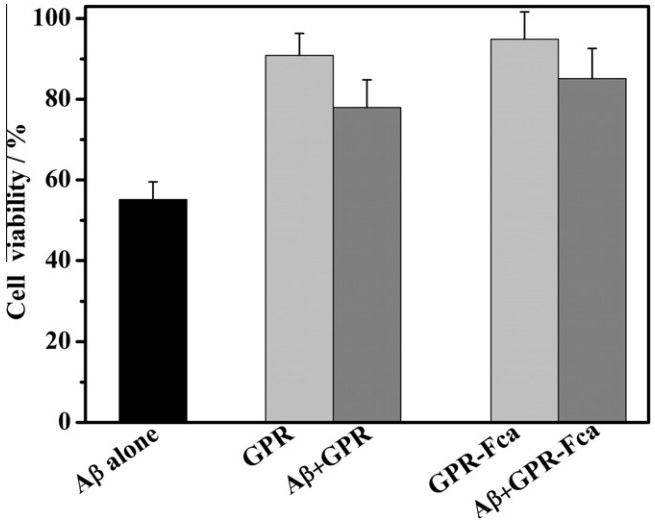

Figure 6. SH-SY5Y cell viabilities in the presence of different solutions. All the added solutions were pre-incubated for 48 h at 32 °C. The cell viability was determined at 24 h after the addition of pre-incubated solutions. The error bars correspond to relative standard deviation values determined from measurements conducted on three different days.

2.8. Enzymatic stability and lipophilicity of GPR and ferrocene GPR conjugates

A major drawback with the use of peptides as drugs in central nervous system diseases is their rapid degradation by proteolytic enzymes. For example, Molineaux and coworkers showed that the use of cholyl–LVFFA as a therapeutic agent is restricted by its propensity to be cleared up completely after the hepatic first pass.[40] One of our aims to modify the GPR peptide with ferrocene moiety is to improve the proteolytic stability of GPR in blood stream. The proteolytic stability of GPR and ferrocene GPR conjugates were studied by HPLC method. As shown in Figure 7, after 24 h incubation at 25 °C, only 20% of intact GPR was detected, while, 45% and 50% of Fc–GPR and GPR–Fca remain intact, respectively. The results are consistent with the experimental hypothesis, that is, the ferrocene tethered GPRs exhibit significantly resistance to proteolytic degradation in comparison with their parent peptide GPR.

It is worth noting that lipophilicity is the most important factor in determining the permeability of drug candidates and plays a dominant role in toxicity predictions.[41] It is well known that ferrocene possess a high lipophilicity and our previous studies demonstrated that the conjugation of ferrocene group to KLVFF peptide results in an increase in the lipophilic value of Fc–KLVFF.[25] In this study, the octanol/water partition coefficient (log *P* value) was used to describe the lipophilicity of the inhibitors. To determine the lipophilicity of GPR–Fca and GPR, log k_w values of all compounds were determined by RP–HPLC and then converted to log *P* value by comparison to reference compounds.[42] As listed in Table 1, the attachment of ferrocene to GPR leads to an increase in the lipophilicity of GPR–Fca compared to parent GPR. Metzler-Nolte and co-workers found that the conjugation of ferrocene moiety to a hydrophilic peptide lead to an increase in lipophilicity thus enhancing the permeation coefficient of peptide across the blood–brain barrier (BBB).[43] Thus, We are inclined to infer that the membrane permeability of GPR would be improved by the conjugation of ferrocene.

3. Conclusions

The ferrocene GPR conjugates were synthesized successfully. The synthesized GPR–Fca shows high inhibitory effect upon $A\beta_{1-}$

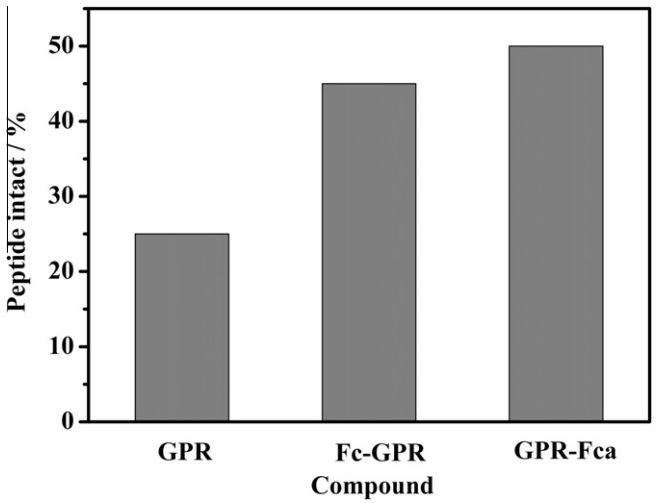

Figure 7. Resistance to proteolytic degradation of GPR and ferrocene GPR conjugates. Aliquots of GPR, GPR–Fca and Fc–GPR at a concentration of 0.76 mg mL^{-1} in 0.1 M PBS were incubated overnight with 0.1 mg mL^{-1} of chymotrypsin at 25 °C. The percentage of the compounds resistant to proteolysis was determined by comparing to the original intact peptide by HPLC.

Table 1
Octanol/water partition coefficients of GPR–Fca and GPR[a]

Compound	Log k_w	Log P
GPR–Fca	2.97	3.15
GPR	1.79	2.01

[a] Log P and log k_w was determined by standard method.[43,44]

$_{42}$ fibril formation and can lead to the disaggregation of existing $A\beta_{1-42}$ mature fibrils. Moreover, the MTT cytotoxicity results indicate that GPR–Fca can effectively inhibit Aβ-induced toxicity towards human neuroblastoma SH-SY5Y cells in vitro. The attachment of ferrocene moiety onto GPR tripeptide allows us to investigate the kinetics of the process that disrupts the $A\beta_{1-42}$ aggregation pathway. And our results suggest that the inhibitory effect is realized through a strong interaction between GPR–Fca and $A\beta_{1-42}$ at the very beginning of incubation. In particular, the good lipophilicity and high resistance to proteolytic degradation of GPR–Fca makes it possible to resist $A\beta_{1-42}$ fibril formation and prevent the Aβ-induced cytotoxicity in vivo. Our results suggest that GPR–Fca is a potential candidate for therapeutic treatment of AD. To develop these inhibitors for the practical treatment of AD in the near future, we are trying to evaluate their pharmacological and therapeutic properties on in vivo animal models, and to improve their efficacy across BBB by modifying their chemical structure or apply new techniques such as nanoparticulate drug delivery systems if necessary.

4. Materials and methods

4.1. Materials

Sodium hydrogen phosphate, sodium dihydrogen phosphate, thioflavine T (ThT) and hexafluoroisopropanol (HFIP) were purchased from Sigma (St Louis, MO). *o*-(Benzotriazol-1-yl)-*N*,*N*,*N*′,*N*′-tetramethyluronium (HBTU) and 1-hydroxybenzotrizole (HOBt) were acquired from HighFine Biotech Co. (Shuzhou, China). Amino acids, Boc-Gly-OH, H-Pro-OMe, Boc-Arg(NO_2)-OH, and H-Arg(NO_2)-OMe were purchased from GL Biochem (Shanghai, China). Triethylamine (Et_3N) and ferrocene (Fc) were obtained from Boer Chemical Reagents Co. (Shanghai, China). Dichloromethane (CH_2Cl_2) obtained from Hengxing (Tianjin, China) was dried and distilled over CaH_2 before use. SH-SY5Y cell (human neuroblastoma) was purchased from American Type Culture Collection Inc. (Manassas, VA). Fetal bovine serum (FBS), Dulbecco's modified Eagle medium (DMEM), Ham's F12 medium were obtained from HyClone (Logan, UT), and the mixture of penicillin and streptomycin was from Sigma (St. Louis, MO). All chemicals were of analytical grade and used without further purification.

4.2. Characterization of compounds

FT-IR spectra of all compounds prepared in KBr pellets were recorded with AVATAR360 Fourier transform spectrophotometer. ^1H NMR spectra were recorded on a Bruker AMX-500 Spectrometer with Me_4Si (TMS) as internal standard. Chemical shifts were reported in ppm relative to TMS for ^1H NMR spectra. Electrospray ionization mass spectrometry (ESI-MS) was conducted on a Thermal Fisher LTQ linear ion-trap mass spectrometer (San Jose, CA).

4.3. Synthesis of GPR, ferrocene monocarboxylic acid (Fc-COOH) and Fca

Tripeptide GPR was synthesized following our previous procedures by standard peptide synthesis procedure in solution using HOBt and HBTU as coupling reagents.[44] Fc-COOH and Fca were synthesized according to the literature procedure.[26,27]

4.4. Synthesis of GPR–Fca (4)

GPR–Fca was synthesized according to the literature procedure,[27,45] and the synthetic procedure was shown in Scheme 1. Briefly, to a solution of Boc-Gly-OH (5 mmol, 1.25 g) in dry CH_2Cl_2 (DCM) at 0 °C, HOBt (5.5 mmol, 0.79 g) and HBTU (5.5 mmol, 2.1 g) were added. After stirring for 1 h at 0 °C, H-Pro-OMe (5 mmol, 0.84 g) by treatment with Et_3N in DCM was added. The reaction mixture was then stirred overnight, and washed with saturated aqueous solutions of $NaHCO_3$, citric acid (10%), and water, then dried over Na_2SO_4, and evaporated to dryness under reduced pressure. The crude product was purified by flash column chromatography (EtOAc/hexanes = 1:1). Then Boc-Gly-Pro-OMe was treated by NaOH aqueous solution and the free acid Boc-Gly-Pro-OH was given. Similarly to the synthetic procedure of Boc-Gly-Pro-OMe, Boc-Arg(NO_2)-Fc-OMe was synthesized. Then Boc-Arg(NO_2)-Fc-OMe was treated by 50% TFA with DCM and NH_2-Arg(NO_2)-Fc-OMe was given.

To a solution of Boc-Gly-Pro-OH (4.0 mmol, 1.09 g) in dry DCM at 0 °C, Et_3N (4.2 mmol, 0.59 mL), HOBt (4.2 mmol, 0.568 g) and HBTU (4.2 mmol, 1.68 g) were added, reacted 1 h at 0 °C, then 1.7 g H-Arg(NO_2)-Fc-OMe by treatment with Et_3N in THF/DMF was added. The reaction mixture was then stirred overnight, and evaporated to dryness under reduced pressure. The crude product was purified by flash column chromatography (DCM/EtOAc/MeOH = 90:30:1) to give Boc-Gly-Pro-Arg(NO_2)-Fca-OMe (GPR–Fca) (yield 30.6%). IR (KBr, cm^{-1}): 3116, 1149, 825 cm^{-1} (í(Fc)), 1712 cm^{-1} (í(C=O)), 1544 cm^{-1} (í(C–N)), 3376 cm^{-1} (s, N–H), 1246 cm^{-1} (s, C–C), 1284 cm^{-1} (s, C–N), 1069 cm^{-1} (s, C–O–C), 1617 cm^{-1} (í(C=N, Arg)).

^1H NMR for GPR–Fca (500 MHz, $CDCl_3$): δ 8.405–8.426 (d, 1H, NH, Pro) 8.01 (m, 1H, á-NH, Arg), 7.776–7.795 (t, 1H, NH, Gly), 7.54–7.60 (m, 1H, â–NH, Arg), 7.42–7.46 (m, H, C=NH Arg), 5.74 (s, 1H, NH Fc), 4.83 (m, 1H, CH, Pro), 4.81 (s, 4H, 2,2′H, 4,4′H Cp), 4.49 (s, 2H, CH_2, Gly), 4.41–4.42 (m, 2H, CH, Pro and Arg), 4.12 (m, 4H, 3,3′H, 5,5′H Cp), 3.81 (s, 3H, OCH_3, Fc), 2.78 (m, 2H, Arg â–CH_2), 2.55 (m, 2H, Arg ã-CH_2), 1.59 (9H, s, Boc).

ESI-MS for GPR–Fca: m/z calcd for $C_{30}H_{44}N_8O_9Fe$ $[M+2H]^{2+}$: 359.1; found: 359.8.

4.5. Synthesis of Fc–GPR (7)

The synthetic procedure of the Fc–GPR was shown in Scheme 1 following our previous work.[44] Briefly, to a solution of Fc-COOH (5.65 mmol, 1.3 g) in dry DCM at 0 °C, Et_3N (6.19 mmol, 0.87 mL), HOBt (6.19 mmol, 0.84 g) and HBTU (6.19 mmol, 2.4 g) were added, reacted 1 h at 0 °C, then 1 g H-Gly-OMe by treatment with Et_3N in DCM (5 mL) was added. The reaction mixture was then stirred overnight at room temperature, washed with saturated aqueous solutions of $NaHCO_3$, citric acid (10%), and water, and evaporated to dryness under reduced pressure at 40 °C. The crude product (Fc-Gly-OMe) was purified by flash column chromatography (DCM/EtOAc = 2:1). Then Fc-Gly-OMe was treated by NaOH aqueous solution and the free acid Fc-Gly-OH was given. Similarly to the synthesis of Fc-Gly-OMe, Pro-Arg(NO_2)-OMe (3.4 mmol, 1.45 g) was added to the solution of Fc-Gly-OH (3.61 mmol, 1.04 g) in DCM. The mixture was then stirred for 24 h at room temperature. The crude product was purified by flash column chromatography (DCM/EtOAc/MeOH = 90:30:5) to give Fc-Gly-Pro-Arg(NO_2)-OMe (Fc–GPR) (yield 48.5%). IR (cm^{-1}): 1105, 824 cm^{-1} (ν(Fc)), 1740 cm^{-1} (ν(C=O)), 1438 cm^{-1} (ν(C–N)), 3307 cm^{-1} (ν(N–H)), 1539 cm^{-1} (δ(N–H)), 1629 cm^{-1} (ν(C=N, Arg)). ^1H NMR (500 MHz, $CDCl_3$,): ä 8.206(s, 1H, á–NH, Arg),7.38(s, 1H, NH, Gly), 7.021(s, 1H, C=NH, Arg), 4.627(m, 1H, CH, Arg), 4.398(s, 2H, 2,2′H Cp), 4.351(s, 2H, 3,3′ H, Cp), 4.215(s, 2H, Gly), 4.141(s, 5H, Cp), 3.792 (s, 3H, OCH_3, Arg), 3.55 (m, 2H, CH_2, Pro), 3.38 (m, 2H, CH_2, Pro), 2.97∼2.76 (m, 4H, Arg â–CH_2, ã–CH_2).

ESI-MS for Fc–GPR: m/z calcd for $C_{25}H_{33}N_7O_7FeNa$ $[M+Na]^+$: 622.2; found 622.6.

4.6. Preparation of $A\beta_{1-42}$ solutions

$A\beta_{1-42}$ purchased from American Peptide Company Inc. (Sunnyvale, CA) was prepared as follows. Briefly, HFIP (250 μL) was added to 0.25 mg of lyophilized $A\beta_{1-42}$ and the solution was kept at room temperature for 2 h. This was followed by sonication for 30 min and then centrifugation at 14,000 rpm for 30 min. The supernatant was pipetted out and freeze-dried. The as-treated $A\beta_{1-42}$ sample was then dissolved in 20 mM NaOH and sonicated for 1 min, which was followed by centrifugation at 14,000 rpm for 30 min. The supernatant was again pipetted out and used to prepare the stock solution of $A\beta_{1-42}$. Ferrocene GPR conjugates were dissolved in DMSO, followed by dilution with water to prepare the stock solution of 1 mM ferrocene GPR conjugates. All aqueous solutions were prepared using Millipore water (18 MΩ cm) treated by a water purification system (Millipore Co., Billerica, MA).

4.7. Fluorometric quantitation of fibrillogenesis

Formation of fibrils was monitored using ThT fluorescence assay. Briefly, an aliquot of the aggregated $A\beta_{1-42}$ from the stock was collected at indicated time intervals and treated with 10 μM ThT in 50 mM glycine–NaOH (pH 9.2) solution immediately before the measurement. ThT fluorescence was measured at 482 nm with excitation at 450 nm and slits of 5 nm for both excitation and emission using an F-2500 FL Spectrophotometer (Hitachi) in a 1.0 cm quartz cuvette.

4.8. Electrochemical measurements

Electrochemical measurement was carried out with a model CHI660B Electrochemical Workstation (CH Instruments, Austin TX) at room temperature. Glassy carbon was the working electrode (diameter 3 mm), platinum wire was the counter electrode, and Ag/AgCl/3.0 M KCl was used as the reference electrode. Ferrocene GPR conjugates were diluted with 0.1 M PBS (pH 7.4) to a final concentration of 50 μM. For differential pulse voltammetric (DPV) determinations, the following conditions were used: sample width 17 ms, pulse amplitude 50 mV, pulse width 50 ms and pulse period 200 ms.

4.9. Atomic force microscopy

The morphology of $A\beta_{1-42}$ aggregates was obtained on a PicoScan SPM microscope (Molecular Imaging, Phoenix, AZ, USA) using a MAC Mode. For imaging, aliquots of $A\beta_{1-42}$ or $A\beta_{1-42}$/GPR–Fca (10 μL) were taken out at a predetermined incubation time and cast onto these mica sheets that had been pretreated with Ni(II) in 10 mM $NiCl_2$ for 15 min. Afterwards, the slides were gently rinsed with water to remove salt, and then dried with N_2.

4.10. Cytotoxicity assay

SH-SY5Y cells were maintained in a medium of DMEM, Ham's F12, FBS, and the mixture of penicillin and streptomycin (V/V/V/V = 44.5%:44.5%:10%:1%) at 37 °C under a humidified atmosphere of 5% CO_2. The cultured cells were then transferred to a 96-well plate with approximately 10,000 cells per well. After overnight incubation at 37 °C the medium was replaced with a DMEM/F12 medium containing 5% FBS and $A\beta_{1-42}$ sample or $A\beta_{1-42}$/GPR, $A\beta_{1-42}$/GPR–Fca mixture which were pre-incubated at 32 °C for 48 h to form the different aggregates, then the SH-SY5Y cells were incubated with the resultant media at 37 °C in an atmosphere of 5% CO_2 for 24 h. Viability of the cells exposed to each solution was determined based on the 3-[4,5-dimethylthiazol-2-yl]-2,5-diphenyltetrazolium bromide (MTT) assay. Briefly, media with the $A\beta_{1-42}$ sample or inhibitor/$A\beta_{1-42}$ mixture in the wells were replaced with 100 μL media containing 0.5 mg mL^{-1}. MTT and the resultant solutions were incubated for 4 h. After removal of the MTT-containing media, 150 μL of DMSO was added into each well to dissolve the formazan precipitate. UV–Vis absorption was then recorded at 570 nm using a microplate reader (Tecan, San Jose, CA). MTT assay in five separate wells was conducted, and the reported viability was the average value obtained on three different days.

4.11. Protease-resistance assay

Aliquots of GPR, GPR–Fca and Fc–GPR at a concentration of 0.76 mg mL^{-1} in 0.1 M phosphate buffered saline (PBS) were incubated overnight with 0.1 mg mL^{-1} of chymotrypsin (Bio Basic Inc., NY, USA) at 25 °C. Thereafter, the samples were injected to reverse-phase HPLC (Shimadzu 6AD, Columbia, MO) on a C18 column (dimension of 250 × 4.6 mm i.d.) from Phenomenex (Torrance, CA) with a linear gradient of 10–50% acetonitrile containing 0.1% trifluoroacetic acid in 20 min. The percentage of the compounds resistant to proteolysis was measured by comparing the peak area (UV absorbance at 215 nm) corresponding to the intact compound which was incubated in PBS.

4.12. Determination of the octanol/water partition coefficient (log$P$ value) by RP-HPLC

Log$P$ values were determined by RP-HPLC according to a literature procedure.[42,43] Water and methanol each containing 0.1% (v/v) TFA were used as eluents. Four different standards with known log$P$ (naphthalene, phenol, acetophenone and nitrophenol) were used for calibrating the system and to establish a correlation be-

tween log$P$ and logk_w. These compounds were dissolved in methanol and uracil was exploited to determine the system's dead time.

Acknowledgments

Partial support of this work by the Natural Science Foundation of China (Nos. 20876179 and 21076232 to Y.L., and 20904066 to J.L.).

Supplementary data

Supplementary data associated with this article can be found, in the online version, at http://dx.doi.org/10.1016/j.bmc.2012.11.030.

References and notes

1. Tabert, M. H.; Liu, X. H.; Doty, R. L.; Serby, M.; Zamora, D.; Pelton, G. H.; Marder, K.; Albers, M. W.; Stern, Y.; Devanand, D. P. *Ann. Neurol.* **2005**, *58*, 155.
2. Brookmeyer, R.; Johnson, E.; Ziegler-Graham, K.; Arrighi, H. M. *Alzheimers Dement.* **2007**, *3*, 186.
3. Lukas, A.; Schuler, M.; Fischer, T. W.; Gibson, S. J.; Savvas, S. M.; Nikolaus, T.; Denkinger, M. Z. *Gerontol. Geriatr.* **2012**, *45*, 45.
4. Allen, P. B.; Chiu, D. T. *BBA Mol. Basis Dis.* **2008**, *1782*, 326.
5. Parker, M. H.; Chen, R.; Conway, K. A.; Lee, D. H. S.; Luo, C.; Boyd, R. E.; Nortey, S. O.; Ross, T. M.; Scott, M. K.; Reitz, A. B. *Bioorg. Med. Chem.* **2002**, *10*, 3565.
6. Doig, A. J. *Curr. Opin. Drug Disc. Dev.* **2007**, *10*, 533.
7. Soto, C.; Castano, E. M.; Frangione, B.; Inestrosa, N. C. *J. Biol. Chem.* **1995**, *270*, 3063.
8. Tjernberg, L. O.; Naslund, J.; Lindqvist, F.; Johansson, J.; Karlstrom, A. R.; Thyberg, J.; Terenius, L.; Nordstedt, C. *J. Biol. Chem.* **1996**, *271*, 8545.
9. Tomiyama, T.; Shoji, A.; Kataoka, K.; Suwa, Y.; Asano, S.; Kaneko, H.; Endo, N. *J. Biol. Chem.* **1996**, *271*, 6839.
10. Iversen, L. *Nature* **2002**, *417*, 231.
11. Yan, J.-W.; Li, Y.-P.; Ye, W.-J.; Chen, S.-B.; Hou, J.-Q.; Tan, J.-H.; Ou, T.-M.; Li, D.; Gu, L.-Q.; Huang, Z.-S. *Bioorg. Med. Chem.* **2012**, *20*, 2527.
12. Sun, Y.; Zhang, G.; Hawkes, C. A.; Shaw, J. E.; McLaurin, J.; Nitz, M. *Bioorg. Med. Chem.* **2008**, *16*, 7177.
13. Reches, M.; Porat, Y.; Gazit, E. *J. Biol. Chem.* **2002**, *277*, 35475.
14. Ashmarin, I. P. *Neurochem. J.* **2007**, *1*, 173.
15. Falalyeyeva, T. M.; Samonina, G. E.; Beregovaya, T. V.; Andreeva, L. A.; Dvorshchenko, E. A. *Bull. Exp. Biol. Med.* **2010**, *149*, 699.
16. Ioudina, M.; Uemura, E. *Exp. Neurol.* **2003**, *184*, 923.
17. Kerman, K.; Kraatz, H.-B. *Analyst* **2009**, *134*, 2400.
18. Bincoletto, C.; Tersariol, I. L. S.; Oliveira, C. R.; Dreher, S.; Fausto, D. M.; Soufen, M. A.; Nascimento, F. D.; Caires, A. C. F. *Bioorg. Med. Chem.* **2005**, *13*, 3047.
19. Dive, D.; Biot, C. *ChemMedChem* **2008**, *3*, 383.
20. Chantson, J. T.; Falzacappa, M. V. V.; Crovella, S.; Metzler-Nolte, N. *J. Organomet. Chem.* **2005**, *690*, 4564.
21. Metzler-Nolte, N. *Chimia* **2007**, *61*, 736.
22. Biot, C. *Curr. Med. Chem.: Anti-Infect. Agents* **2004**, *3*, 135.
23. Biot, C.; Taramelli, D.; Forfar-Bares, I.; Maciejewski, L. A.; Boyce, M.; Nowogrocki, G.; Brocard, J. S.; Basilico, N.; Olliaro, P.; Egan, T. *J. Mol. Pharm.* **2005**, *2*, 185.
24. Top, S.; Vessieres, A.; Leclercq, G.; Quivy, J.; Tang, J.; Vaissermann, J.; Huche, M.; Jaouen, G. *Chem. Eur. J.* **2003**, *9*, 5223.
25. Wei, C.-W.; Peng, Y.; Zhang, L.; Huang, Q.; Cheng, M.; Liu, Y.-N.; Li, J. *Bioorg. Med. Chem. Lett.* **2011**, *21*, 5818.
26. Barisic, L.; Rapic, W.; Kovac, V. *Croat. Chem. Acta* **2002**, *75*, 199.
27. Barisic, L.; Rapic, V.; Metzler-Nolte, N. *Eur. J. Inorg. Chem.* **2006**, 4019.
28. Barisic, L.; Cakic, M.; Mahmoud, K. A.; Liu, Y.-N.; Kraatz, H.-B.; Pritzkow, H.; Kirin, S. I.; Metzler-Nolte, N.; Rapic, V. *Chem. Eur. J.* **2006**, *12*, 4965.
29. Hamels, D.; Dansette, P. M.; Hillard, E. A.; Top, S.; Vessieres, A.; Herson, P.; Jaouen, G.; Mansuy, D. *Angew. Chem., Int. Ed.* **2009**, *48*, 9124.
30. Chavain, N.; Vezin, H.; Dive, D.; Touati, N.; Paul, J.-F.; Buisine, E.; Biot, C. *Mol. Pharm.* **2008**, *5*, 710.
31. LeVine, H. *Methods Enzymol.* **1999**, *309*, 274.
32. Sciarretta, K. L.; Gordon, D. J.; Meredith, S. C. In *Methods Enzymology*; Kheterpal, I., Wetzel, R., Eds.; 2006; Vol. 413, pp 273 312.
33. Bett, C. K.; Ngunjiri, J. N.; Serem, W. K.; Fontenot, K. R.; Hammer, R. P.; McCarley, R. L.; Garno, J. C. *ACS Chem. Neurosci.* **2010**, *1*, 608.
34. Soto, C.; Kindy, M. S.; Baumann, M.; Frangione, B. *Biochem. Biophys. Res. Commun.* **1996**, *226*, 672.
35. Lou, H.; Fan, P.; Perez, R. G.; Lou, H. *Bioorg. Med. Chem.* **2011**, *19*, 4021.
36. Pallitto, M. M.; Ghanta, J.; Heinzelman, P.; Kiessling, L. L.; Murphy, R. M. *Biochemistry* **1999**, *38*, 3570.
37. Lowe, T. L.; Strzelec, A.; Kiessling, L. L.; Murphy, R. M. *Biochemistry* **2001**, *40*, 7882.
38. Austen, B. M.; Paleologou, K. E.; Ali, S. A. E.; Qureshi, M. M.; Allsop, D.; El-Agnaf, O. M. A. *Biochemistry* **1984**, *2008*, 47.
39. Yao, D.; Zhang, F. G.; Yu, L. N.; Yang, Y. N.; van Breemen, R. B.; Bolton, J. L. *Chem. Res. Toxicol.* **2001**, *14*, 1643.
40. Findeis, M. A.; Lee, J. J.; Kelley, M.; Wakefield, J. D.; Zhang, M. H.; Chin, J.; Kubasek, W.; Molineaux, S. M. *Amyloid* **2001**, *8*, 231.
41. Crivori, P.; Cruciani, G.; Carrupt, P. A.; Testa, B. *J. Med. Chem.* **2000**, *43*, 2204.
42. Minick, D. J.; Frenz, J. H.; Patrick, M. A.; Brent, D. A. *J. Med. Chem.* **1923**, *1988*, 31.
43. Pinto, A.; Hoffmanns, U.; Ott, M.; Fricker, G.; Metzler-Nolte, N. *ChemBioChem* **1852**, *2009*, 10.
44. Liu, X.-F.; Li, X.-Q.; Ye, W.-L.; Zhou, B.-B.; Liu, Y.-N. *Acta Phys. Chim. Sin.* **2010**, *26*, 2381.
45. Moriuchi, T.; Nomoto, A.; Yoshida, K.; Ogawa, A.; Hirao, T. *J. Am. Chem. Soc.* **2001**, *123*, 68.